DRD No. SE-7
DRL No. 58

SILICON MATERIALS TASK OF THE LOW COST SOLAR ARRAY PROJECT (PHASE III)

Dist. Category UC-63
DOE/JPL-954331-79/1

Effect of Impurities and Processing on Silicon Solar Cells

Thirteenth Quarterly Report

January, 1979

October 1978-December 1978

R. H. Hopkins, J. R. Davis, P. D. Blais,
A. Rohatgi, R. B. Campbell and P. Rai-Choudhury
Westinghouse Research & Development Center
and
H. C. Mollenkopf and J. R. McCormick
Dow Corning Corporation

Contract No. 954331

The JPL Low Cost Silicon Solar Array Project is sponsored by the U. S. Dept. of Energy and forms part of the Solar Photovoltaic Conversion Program to initiate a major effort toward the development of low-cost solar arrays. This work was performed for the Jet Propulsion Laboratory, California Institute of Technology by agreement between NASA and DOE.

Westinghouse R&D Center
1310 Beulah Road
Pittsburgh, Pennsylvania 15235

TABLE OF CONTENTS

TECHNICAL CONTENT STATEMENT

This report was prepared as an account of work sponsored by the United States Government. Neither the United States nor the United States Department of Energy, nor any of their employees, nor any of their contractors, sub-contractors, or their employees,makes any warranties, express or implied, or assumes any legal liability or responsibility for the accuracy, completeness or usefulness of any information, apparatus, product or process disclosed, or represents that its use would not infringe privately owned rights.

NEW TECHNOLOGY

No new technology is reportable for the period covered by this report.

1. SUMMARY

This is the 13th quarterly report of a study entitled an Investigation of the Effects of Impurities and Processing on Silicon Solar Cells. The objective of the program is to define the effects of impurities, various thermochemical processes and any impurity-process interactions on the performance of terrestrial silicon solar cells.

The Phase III program effort falls in five areas: (1) cell processing studies (2) completion of the data base and impurity-performance modeling for n-base cells (3) extension of p-base studies to include contaminants likely to be introduced during silicon production, refining or crystal growth (4) anisotropy effects and (5) a preliminary study of the permanence of impurity effects in silicon solar cells. The focus of this quarter's activity was tasks on (1), (3) and (4).

Gettering experiments with phosphorus oxychloride gas phase treatments at 950°C, 1000°C, and 1150°C have been completed for two Ti-doped ingots ($3x10^{13}$ cm^{-3} and $2.1x10^{14}$ cm^{-3} Ti doping levels, respectively), two molybdenum doped ingots ($8x10^{11}$ and $4.2x10^{12}$ cm^{-3} Mo) and one iron-doped ingot ($3x10^{14}$ cm^{-3} Fe). For the Ti and Fe ingots two clear trends were observed: (1) at any fixed temperature, e.g. 1100°C, as gettering time was extended cell performance improved; (2) as gettering temperature was increased at fixed heat treatment time cell performance also improved. For example, in these experiments the maximum improvement for the $3x10^{13}$ cm^{-3} Ti ingot occurred after 4 hours at 1100°C: the cell efficiency was raised to 77% of the undoped baseline from an initial untreated value of 57% of baseline. The iron-doped ingot recovered to 100% of the baseline cell value from the untreated value of 82%. (A small decline in baseline efficiency at the higher temperature was noted). Little or no improvement on the cell performance of the Mo-doped ingots was obtained.

First generation Co and W-doped ingots were grown and processed to solar cells. Neither dopant could be detected in the ingots by spark source mass spectroscopy (SSMS) although depreciation in cell performance occurred in each case. The detection limits of the SSMS place an upper limit on the segregation coefficients at about 10^{-5} and 10^{-6} for Co and W respectively. W reduces cell performance by degrading bulk lifetime; Co like Fe and Cu appears also to affect junction properties.

Miniature solar cells and diodes were used to map the characteristics of wafers from a 3 inch diameter ingot doped with Mn or Ti. Wafers were processed from the seed, center, and tang end of the ingot. The cell performance showed no significant anisotropy or non-uniformity with position in the wafer or ingot. Cell efficiency within a given wafer varied by no more than $\pm$ 5% of the average value. The magnitude of the cell efficiency and OCD lifetimes for the large diameter (commercial size) ingots agreed with the values obtained on our standard 1 inch diameter test ingot. A model has been developed to describe the behavior of solar cells bearing non-uniform distributions of impurities or defects.

2. INTRODUCTION

This is the 13th quarterly report describing activities conducted under JPL Contract 954331. Phase III of this program is entitled an Investigation of the Effects of Impurities and Processing on Silicon Solar Cells.

The objective of this program is to determine how various processes, impurities, and impurity-process interactions affect the properties of silicon and the performance of terrestrial solar cells made from silicon. The development of this data base permits the definition of the tolerable impurity levels in a low-cost Solar Grade Silicon. The data further provide the silicon manufacturer with a means to select materials of construction which minimize product contamination and permit the cost-effective selection of chemical processes for silicon purification. For the silicon ingot, sheet or ribbon manufacturer the data suggest what silicon feedstock purity must be selected to produce wafers suitable for cell production and what furnace materials minimize wafer contamination. The cell manufacturer may use the data to define an acceptable wafer purity for cell processing or to identify processes which minimize impurity impact on efficiency. In short, the data provide a basis for cost-benefit analysis to the producers and users of Solar Grade Silicon.

The program approach has been to evaluate the chemical, microstructural, electrical, and solar cell characteristics of silicon wafers infused with controlled amounts of various metal contaminants. The wafers are produced from Czochralski ingots and silicon web crystals.

The Phase III effort encompasses five major topics: (1) expansion of the activity directed to cell processing (2) completion of the data base and modeling of n-base solar cells (3) extension the p-base studies to include impurities likely to be introduced during silicon

production, refining or crystal growth, (4) a consideration of the potential impact of anisotropic impurity distribution in large Czochralski and ribbon solar cells and (5) a preliminary investigation of the permanence of impurity effects in silicon solar cells. The focus of this quarter's activity was on tasks (1), (3) and (4). Highlights of this effort are described below.

3. TECHNICAL RESULTS

3.1 Ingot Preparation and Evaluation

3.1.1 Ingot Preparation

During this quarter three main types of silicon ingots were prepared: ingots for processing studies, first generation ingots representing materials of construction (cobalt and tungsten), and second and third generation n-base ingots. Eleven ingots were grown and as before each was prepared by the Czochralski Crystal growth method. Details of the crystal growth equipment and conditions can be found in earlier reports (1,2). The ingots prepared this quarter included:

1 p-type singly doped low resistivity (0.2 ohm-cm)
2 p-type singly doped (4 ohm-cm)
6 n-type singly doped (1.5 ohm-cm)
1 p-type high resistivity baseline (30 ohm-cm)
1 p-type singly doped high resistivity (30 ohm-cm)

3.1.2 Ingot Evaluation

The impurity content, electrical resistivity, and etch pit density of each ingot was evaluated as described previously (2,3). Resistivity and etch pit densities for ingots W-129 through W-154 are listed in Table 1. In general, there is no deviation from the established norms [1] for either property.

The effective segregation coefficients used to determine the appropriate ingot melt concentrations are listed in Appendix 7.1. The upper limit values for tungsten and cobalt were recently determined on the basis of mass spectrographic analysis of ingots W-145 and W-146 respectively. The inability to detect tungsten in W-145 and cobalt in

Table 1. Resistivity and Etch Pit Density of Phase III Ingots

Ingot Identification	TGT Resistivity (ohm-cm)	Actual Resistivity (ohm-cm)	Etch Pit Density (/cm^2) +
W-129-00-000(7.6 cm)	4.0 (B)	4.7-3.0	1K-Gross Lineage
W-130-00-000(7.6 cm)	4.0 (B)	4.7-3.7	0K-Gross Lineage
W-131-Mn-008(7.6 cm)	4.0 (B)	6.0-3.8	0K-Gross Lineage
W-132-Ta-003	4.0 (B)	3.8-3.4	1-20K
W-133-00-000	4.0 (B)	4.3-3.7	0K-Gross Lineage
W-134-Ti-009	4.0 (B)	4.9-4.4	0-10K
W-135-Fe-005	4.0 (B)	5.3-2.1	0-Gross Lineage
W-136-Fe-006	4.0 (B)	3.3-2.7	1K-Gross Lineage
W-137-Ti-010	4.0 (B)	4.6-4.4	0-Gross Lineage
W-138-Mo-005	4.0 (B)	5.0-4.1	0-5K
W-139-Mo-006	4.0 (B)	4.0-2.3	0-Gross Lineage
W-140-Ti-011(7.6 cm)	4.0 (B)	3.6-1.7	5K-Gross Lineage
W-141-Mo/Cu-001	4.0 (B)	4.7-3.0	2K-Gross Lineage
W*-142-00-000	0.2 (B)	0.22-0.20	0-3K
W*-143-Ti-002	0.2(B)	0.21-0.15	0-Gross Poly
W*-144-Mo-001	0.2(B)	0.23-0.19	0-Gross Poly
W-145-W-001	4 (B)	4.5-4.0	2K-Gross Poly
W-146-Co-001	4 (B)	4.7-4.2	1K-Gross Poly
W-147-n/Ni-002	1.5(P)	1.9-1.4	2-15K
W-148-N/Mn-002	1.5(P)	2.5-2.1	1K-Gross Poly
W-149-N/Fe-003	1.5(P)	2.0-1.6	3K-Gross Poly
W-150-N/V-003	1.5(P)	2.0-1.5	1-5K
W**-151-00-000	30(B)	35.6-18.1	0-5K
W**-152-Ti-001	30(B)	31.9-25	0-Gross Poly
W-153-N/Ti-003	1.5(P)	2.1-1.1	0-10K
W-154-N/Cr-003	1.5(P)	2.1-1.4	3K-10K

* Use of asterisk indicates low resistivity p-type ingot.

** Use of double asterisk indicates 30 ohm-cm p-type ingot.

\+ The first figure is etch pit density of the seed; second figure etch pit density of extreme tang end of ingot. The first value shown is indicative of dislocation density in slices used for cell fabrication Structural degradation commonly occurs at the tang end of the most heavily-doped ingots due to constitutional supercooling.(1)

W-146 by mass spectrographic analysis placed upper limits on the intended dopant concentrations. Target concentrations, calculated concentrations based on melt analysis, measured impurity concentrations based on spark source mass spectrographic analysis for all ingots are summarized in Appendix 7.2. Mass spectrographic analysis and atomic absorption data comparisons, when applicable, continue to agree within the expected limits of error. A best estimate of the impurity concentration for each Phase III ingot is compiled in Table 2.

The detectability of cobalt in a silicon spectrum by mass spectroscopy is hindered by the intense silicon background produced by the lines of Si^+ at m/e = 28 and 29. The most intense cobalt line at m/e = 59 corresponds to a line of Si^+_2. The next most intense line of cobalt at m/e = 29 1/2 is masked by intense lines of Si^+ at m/e = 28 and 29. Using the limit of detectability at 0.033 ppma cobalt (1.7×10^{15} atoms/cm^3). The least intense line of cobalt at m/e = 19 2/3 is masked by the lines of Si^{2+} at m/e = 14, 14 1/2 and 15. The cobalt line at m/e = 19 2/3 is also 3 times less intense than the line of cobalt at m/e = 29 1/2. Since we could not detect cobalt at a concentration less than 1.7×10^{15} atoms/cm^3 when the melt concentration was 1.5×10^{20} atoms/cm^3 this placed an upper limit for the cobalt effective segregation coefficient of 1.1×10^{-5}.

Tungsten in W-145 was not detectable at a concentration of 0.003 ppma (1.5×10^{14} atoms/cm^3) using the longest mass spectrographic exposure of 1000 coulombs. This concentration limit for the ingot taken with ingot melt concentration of 9.7×10^{19} atoms/cm^3 yields an upper limit for the tungsten effective segregation coefficient of 1.6×10^{-6}.

Carbon and oxygen concentrations of each ingot were measured by infrared absorption. The amplitude of the absorption peak for carbon at 606 cm^{-1} and oxygen at 1107 cm^{-1} wave numbers are proportional to the carbon and oxygen concentrations, respectively. The constants of proportionality used in this work were 2.2 for carbon and 9.6 for oxygen.[2] Normal carbon and oxygen concentrations found in Czochralski grown material are in the range of 2.5×10^{16} atoms/cm^3 to 5×10^{17} atoms/cm^3 for carbon and 50×10^{16} atoms/cm^3 to 150×10^{16} atoms/cm^3 for oxygen. No

Table 2. Best Estimate of Impurity Concentrations of Phase III Ingots

Ingot Identification	Best Estimate of Impurity Conc. (10^{15} atoms/cm^3)
W-129-00-000 (7.6 cm)	NA
W-130-00-000 (7.6 cm)	NA
W-131-Mn-008 (7.6 cm)	0.55
W-132-Ta-003	0.0002
W-133-00-000	NA
W-134-Ti-009	0.05
W-135-Fe-005	1.0
W-136-Fe-006	0.3
W-137-Ti-010	0.21
W-138-Mo-005	0.001
W-139-Mo-006	0.0042
W-140-Ti-011 (7.6 cm)	0.18
W-141-Mo/Cu-001	0.004/4.00
W*-142-00-000	NA
W*-143-Ti-002	0.20
W-144-Mo-001	0.004
W-145-W-001	<0.15
W-146-Co-001	<1.7
W-147-N/Ni-002	0.40
W-148-N/Mn-002	0.60
W-149-N/Fe-003	0.60
W-150-N/V-003	0.03
W**-151-00-000	NA
W**-152-Ti-001	Processing
W-153-N/Ti-003	Processing
W-154-N/Cr-003	Processing

* Low resistivity p-type ingot identification

** 30 ohm-cm p-type ingot identification

Table 3. Carbon and Oxygen Concentrations of Phase III Ingots

Ingot Number	Carbon Concentration x 10^{16} atoms/cm^3	Oxygen Concentration x 10^{16} atoms/cm^3
W-129-00-000	11.3	202
W-131-Mn-008	5.3	164
W-133-00-000	10.4	117
W-135-Fe-005	9.4	118
W-137-Ti-010	5.3	134
W-139-Mo-006	6.5	149
W-141-Mo/Cu-001	8.3	156
W*143-Ti-002	++	++
W-145-W-001	5.8	149
W-147-N/Ni-002	14.0	157
W-149-N/Fe-003	6.6	151
W**151-00-000 (30Ω-cm)	7.0	154
W-153-N/Ti-001	7.5	160

* low resistivity ingot

** high resistivity ingot

++ Due to free carrier absorption infrared methods cannot be used for carbon and oxygen determination in these samples.

significant variations from these values were observed in the ingots produced this quarter as indicated by the data for the odd numbered ingots listed in Table 3.

3.2 Processing Studies

A sizeable portion of this impurity-interaction study is directed toward investigating the effect of several thermochemical processes on the cell performance of impurity-doped silicon. These thermochemical processes are those which can be performed on the doped ingot to reduce the harmful effects of metal contamination.

The program plan called for studying three impurities at two different impurity levels[1] ingots. One iron ingot produced was not suitable for processing due to cellular breakdown during growth so a total of 5 ingots have been studied so far.

The thermochemical processes under study are: (1) $POCl_3$ gettering, (2) HCl gettering and (3) damage gettering. These processes are thermally activated. Thus, it should be possible to characterize each by time, temperature and activation energy so that the results may be extrapolated as to impurity level and gettering cycles.

The processing chart and the experimental plan were presented in Figures 1 and 2 of one Twelfth Quarterly Report[4]. Thus far, we have completed all of the $POCl_3$ gettering experiments on the five ingots as indicated below.

The $POCl_3$ gettering steps were:

Isochronal	1 hr. - 950°C
	1 hr. - 1000°C
	1 hr. - 1100°C
Isothermal	2 hrs. - 1100°C
	3 hrs. - 1100°C
	5 hrs. - 1100°C

The ingots studied were:

136 Fe 006 (3×10^{14} Fe)
134 Ti 009 (5×10^{13} Ti)
137 Ti 010 (2.1×10^{14} Ti)

138Mo005 (1 x 10^{12}Mo)
139 Mo006 (4.2 x 10^{12} Mo)

The data for these five ingots is compiled in Tables 4 through 8 and presented in graphical form in Figures 1 and 2. Figure 1 illustrates the results of the isochronal treatments with the log $\frac{\eta \text{ ingot}}{\eta \text{ base}}$ plotted vs time at 1100°C.

Several comments are appropriate with respect to the data. In Tables 4, 5, and 6, the baseline cell efficiency (and other baseline parameters) show a gentle decrease with increased treatment temperature. This is in general agreement with previous results [1]. These results reveal that the recombination lifetime of the baseline samples reached a weak maximum after 1 gettering cycle (1 hr. at 1000°C in $POC\ell_3$) and further getter cycles caused a slight decline in lifetime. (A similar degrading effect was noted in doped ingot at that time. We did not observe this in the present work and the reasons for such partial disparity in results are now being explored). It may be that two competing mechanisms are operative during gettering of the doped ingots. The first may be a simple diffusion of contaminants to the surface where they are removed, and a second, yet to be understood phenomena may be one by which increased gettering degrades the cell parameters. In any case, the final value of the baseline parameters would set an effective limit on the maximum improvement that may be expected when gettering a doped ingot.

The iron ingot (W136) exhibited a complete recovery to baseline properties, i.e., $\eta_I/\eta_B \approx 1.0$, after gettering. The result is somewhat misleading. Although the cell efficiency of the iron ingot improved from about 8.2% to $\approx$ 9%, the baseline decreased from 10% to below 9%. Thus, in absolute terms, the iron ingot only recovered about 40% of that required to match the original baseline properties.

For the two Mo ingots (138 and 139) gettering produced only slight improvements (and then only at 1100°C) in cell efficiency compared to the untreated material. It must tentatively be concluded that $POC\ell_3$

TABLE 4

$POCl_3$ GETTERING EXPERIMENT — BASELINE - W11700-000

INGOT - W136FE006 ($3x10^{14}$ Fe)

TREATMENT		I_{SC}(mA)	V_{OC}(V)	FF	EFF(%)
None	B	22.6	.559	.749	10.00
1	I	20.0	.536	.725	8.23
	I/B	.887	.959	.968	.824
1HR-950°C	B	21.8	.551	.739	9.36
2	I	21.5	.552	.717	9.03
	I/B	.986	1.00	.970	.965
1HR-1000°C	B	21.4	.549	.726	8.99
3	I	21.7	.549	.720	9.13
	I/B	1.01	1.00	.992	1.01
1HR-1100°C	B	21.2	.541	.693	8.41
4	I	21.3	.546	.684	8.40
	I/B	1.00	1.01	.987	1.00
2HR-1100°C	B	21.1	.546	.690	8.38
5	I	21.4	.555	.737	9.24
	I/B	1.04	1.02	1.07	1.10
3HR-1100°C	B	21.3	.544	.715	8.77
6	I	21.6	.553	.735	9.34
	I/B	1.01	1.02	1.03	1.06
5HR-1100°C	B	21.3	.546	.702	8.63
7	I	21.4	.555	.719	8.98
	I/B	1.01	1.02	1.02	1.04

TABLE 5

$POCl_3$ GETTERING EXPERIMENT (AVERAGE VALUES)

BASELINE - W11700-000
INGOT - W134Ti009 ($5x10^{13}$Ti)

TREATMENT		I_{SC}(mA)	V_{OC}(V)	FF	EFF(%)
None	B	22.40	.556	.729	9.60
1	I	15.42	.491	.694	5.56
	I/B *	.689	.882	.953	.579
1HR-950°C	B	21.30	.549	.729	8.98
2	I	15.36	.484	.699	5.30
	I/B	7.21	.882	.937	.590
1HR-1000°C	B	21.34	.550	.746	9.25
3	I	15.68	.492	.699	5.69
	I/B	.735	.895	.937	.615
1HR-1100°C	B	21.20	.545	.715	8.74
4	I	16.20	.500	.700	5.99
	I/B	.764	.917	.979	.685
1HR-1100°C	B	21.65	.549	.741	9.32
5	I	16.98	.505	.706	6.41
	I/B	.784	.920	.953	.688
3HR-1100°C	B	21.67	.546	.720	9.01
6	I	17.06	.505	.697	6.35
	I/B	.787	.925	.968	.705
5HR-1100°C	B	21.50	.543	.706	8.73
7	I	17.58	.513	.702	6.71
	I/B	8.18	.945	.994	.769

* I/B = value of the property divided by that for the baseline ingot.

TABLE 6

$POCl_3$ GETTERING EXPERIMENT (AVERAGE VALUES)

BASELINE - W11700-000

INGOT - W137Ti-010 (2.1×10^{14} Ti)

TREATMENT		I_{SC} (mA)	V_{OC} (V)	FF	EFF (%)
None	B	22.35	.557	.753	9.91
1	I	12.63	.463	.686	4.24
	I/B	.565	.831	.911	.428
1HR-950°C	B	21.6	.550	.720	9.05
2	I	12.7	.467	.674	4.23
	I/B	.588	.849	.936	.467
1HR-1000°C	B	21.3	.553	.718	8.93
3	I	13.6	.475	.669	4.55
	I/B	.638	.859	.932	.510
1HR-1100°C	B	21.6	.552	.728	9.20
4	I	14.1	.483	.675	4.87
	I/B	.653	.859	.932	.529
2HR-1100°C	B	21.5	.550	.722	9.03
5	I	14.5	.484	.671	5.00
	I/B	.674	.880	.929	.554
3HR-1100°C	B	21.4	.547	.708	8.78
6	I	14.8	.488	.681	5.19
	I/B	.692	.892	.962	.591
5HR-1100°C	B	21.6	.544	.668	8.29
7	I	15.4	.494	.685	5.49
	I/B	.713	.908	1.03	.662

TABLE 7

$POC\ell_3$ GETTERING EXPERIMENT

BASELINE - W117-000

INGOT - W138MO005 ($1x10^{12}$Mo)

TREATMENT		I_{SC}(mA)	V_{OC}(V)	FF	EFF (%)
None	B	22.47	.559	.749	9.95
	I	20.83	.529	.698	8.14
	I/B	.927	.946	.933	.818
1HR/950°C	B	21.57	.546	.699	8.71
	I	19.85	.519	.680	7.40
	I/B	.920	.951	.973	.850
1HR/1000°C	B	21.70	.551	.723	8.67
	I	20.10	.522	.684	7.61
	I/B	.926	.947	.986	.878
1HR/1100°C	B	21.70	.546	.693	8.67
	I	20.23	.520	.683	7.61
	I/B	.932	.957	.986	.878
2HR/1100°C	B	21.40	.549	.702	8.73
	I	20.07	.521	.671	7.62
	I/B	.938	.949	.956	.873
3HR/1100°C	B	21.50	.549	.723	9.02
	I	20.12	.523	.687	7.64
	I/B	.936	.953	.950	.847
5HR/1100°C	B	21.37	.542	.719	8.85
	I	20.17	.523	.756	8.45
	I/B	.944	.965	1.05	.955

TABLE 8

$POC\ell_3$ GETTERING EXPERIMENT

BASELINE - W117-000

INGOT - W139MO006 (4.2×10^{12} Mo)

TREATMENT		I_{SC}(mA)	V_{OC}(V)	FF	EFF (%)
None	B	22.03	.550	.736	9.43
	I	18.43	.507	.688	6.82
	I/B	.837	.922	.935	.723
1HR/950°C	B	21.80	.550	.709	9.00
	I	18.37	.503	.700	6.88
	I/B	.843	.915	.987	.764
1HR/1000°C	B	21.80	.553	.734	9.47
	I	18.43	.505	.695	6.84
	I/B	.843	.915	.947	.722
1HR/1100°C	B	21.80	.545	.700	8.79
	I	18.70	.505	.665	6.65
	I/B	.858	.927	.950	.757
2HR/1100°C	B	22.10	.555	.749	9.71
	I	17.70	.503	.688	6.48
	I/B	.801	.906	.919	.667
3HR/1100°C	B	21.65	.553	.732	9.26
	I	18.98	.509	.701	7.17
	I/B	.877	.920	.958	.774
5HR/1100°C	B	21.80	.551	.747	9.49
	I	18.84	.512	.701	7.15
	I/B	.864	.929	.938	.753

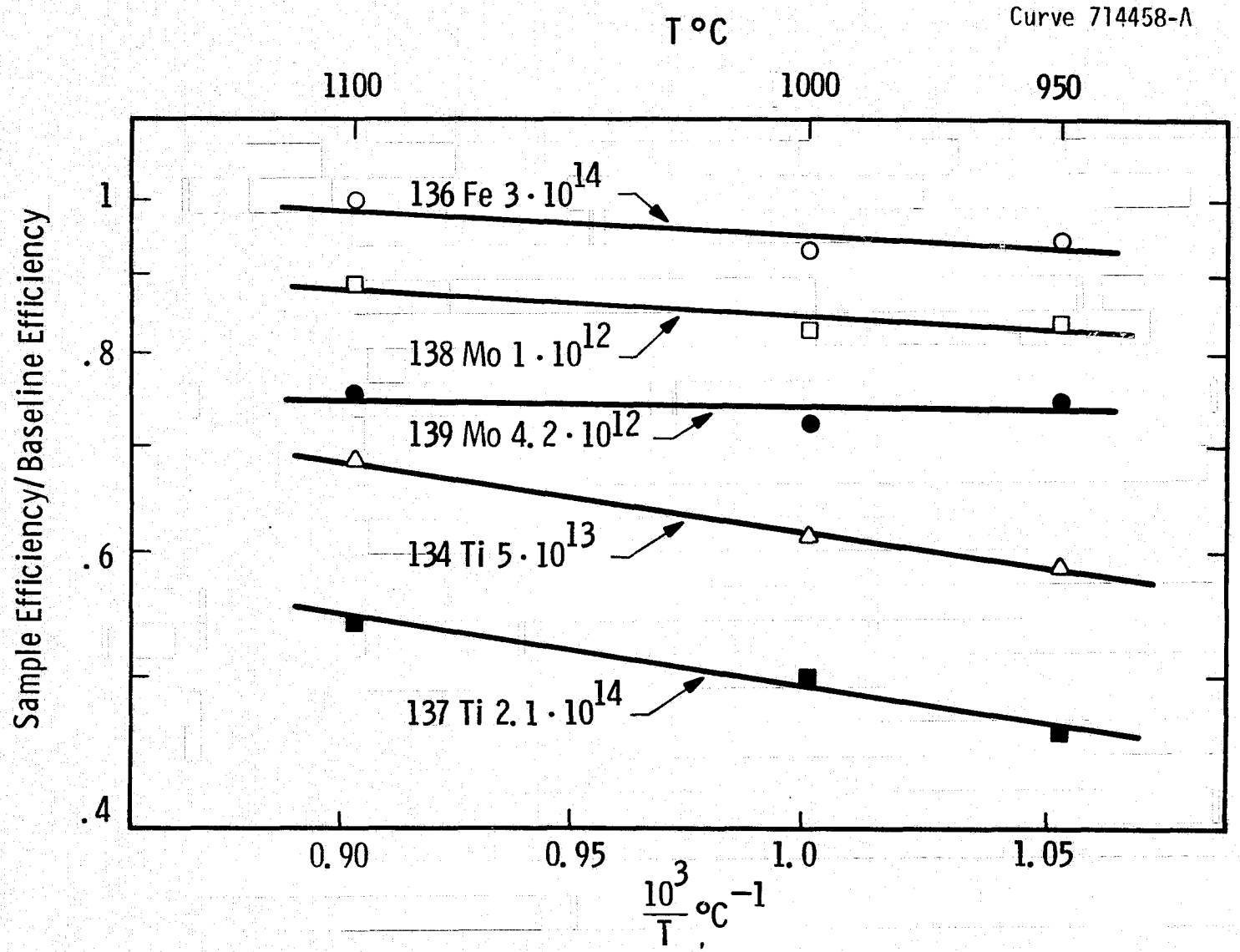

Fig. 1 – Normalized efficiency for isochronal $POCl_3$ gettering (1 hour)

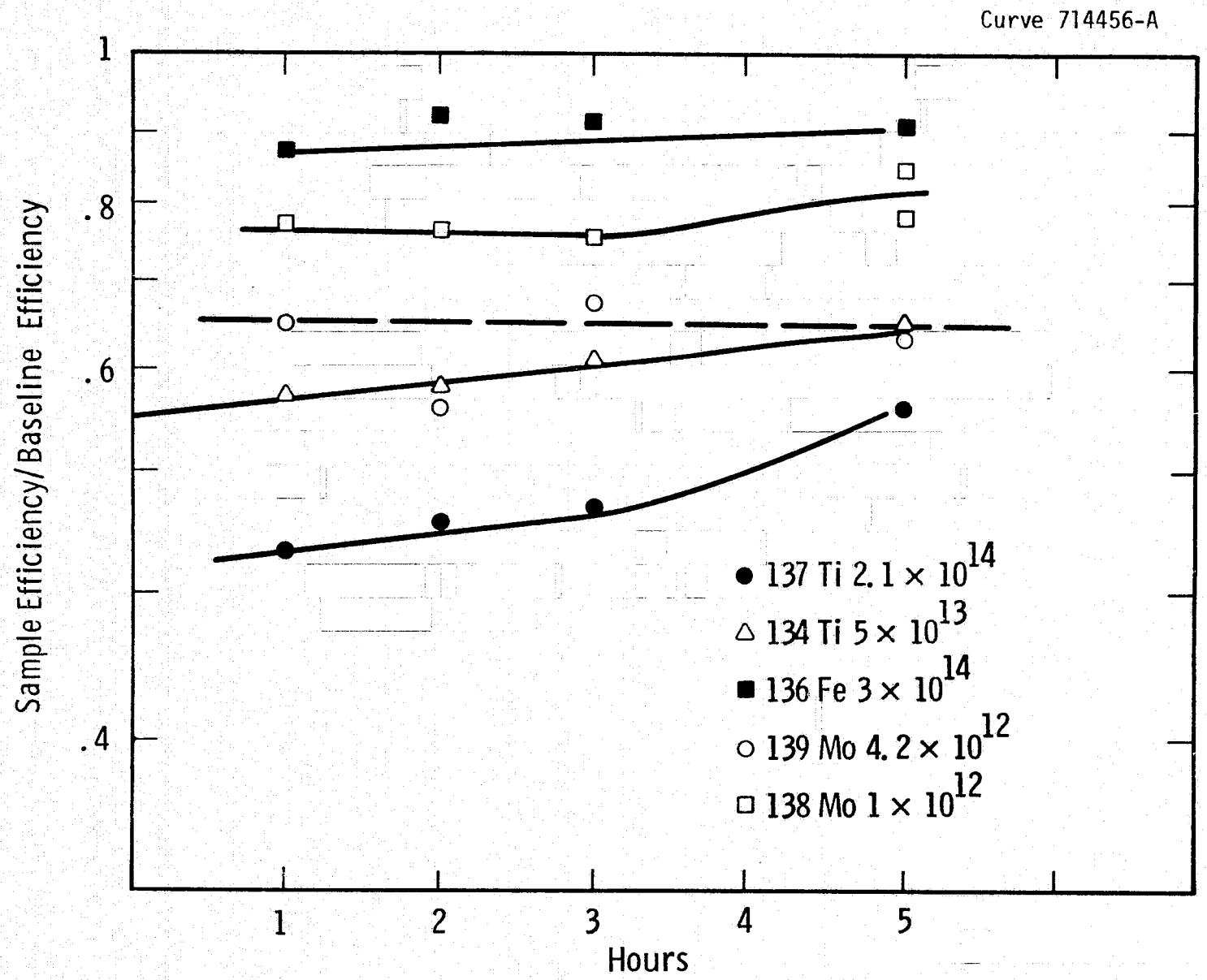

Fig. 2 – Normalized efficiency for isothermal $POCl_3$ gettering (1100°C)

gettering has very little effect on Mo contaminated wafers (at least in impurity range studied so far).

The cell performance of the two Ti ingots show a gradual increase during the gettering cycle, with the normalized efficiency increasing by 0.10 to 0.15. It would appear, however, that abnormally long gettering cycles would be required to achieve anywhere near complete recovery.

From these first $POC\ell_3$ gettering cycles, we can draw the following tentative conclusions:

1. Mo doped ingots are relatively unaffected by $POC\ell_3$ gettering.
2. The cell efficiencies of Ti-doped ingots improve with $POC\ell_3$ gettering but complete recovery to baseline values would appear to require excessive times/temperatures.
3. The ingot with 3×10^{14} Fe doping improves significantly, reaching a maximum of 9.34% efficiency, (after 3 hrs. at 1100°C). This is an improvement of one percentage point in absolute efficiency.
4. The baseline wafers degrade slightly with increasing gettering cycles. This effect may effectively limit any recovery in the ingot.

The results discussed here apply only to $POC\ell_3$ gettering. During the next quarter, data on $HC\ell$ and back surface damage gettering may shed more light on the magnitude of the ultimate recovery in cell properties that can be expected from gettering.

3.3 Effect of Impurities on p-base Silicon Solar Cells

Our studies of impurity effects in p-base solar cells are fairly detailed and complete. The mechanism of cell performance reduction is understood to be primarily lifetime degradation via the introduction of contaminants which form recombination centers in silicon. Device performance can be modeled very accurately on the basis of this

assumption. As a result, cell efficiency as a function of impurity content for p-base devices can now be projected with some confidence.[1] Thus, Phase III activity has been shifted to focus on elements likely to be introduced during silicon production, refining, or crystal growth. As noted in secion 3.1, the first two elements to be investigated are tungsten and cobalt, common components of the refractory hardware used in process equipment and furnaces.

First generation ingots were grown from melts containing the maximum concentration of tungsten or cobalt which could be tolerated without crystal breakdown due to constitutional supercooling. Spark source mass spectroscopy failed to detect either element in the ingot (Secion 3.1) placing upper limits on the tungsten in ingot W145 at $1.7 \times 10^{15} cm^{-3}$ and the cobalt in ingot W146 at 1.5×10^{14} cm^{-3}. The estimated upper limits on the segregation coefficients, 10^{-6} to 10^{-5}, are in the range expected from past experience with other transition metals.[1,2]

Wafers from each ingot were processed into solar cells by the same standard sequence [1,2] involving $POC\ell_3$ diffusion at 825°C that has been employed for all other ingots studied in this program.

The data for tungsten-doped ingot W145, Table 9, shows an average uncoated solar cell efficiency of 8.6% or about 89% of the uncontaminated baseline wafers. We would expect, from the position of tungsten in the periodic table, to observe behavior somewhat similar to that of molybdenum, a strong lifetime killer. The data in Table 9, in fact, show that the efficiencies of the tungsten-doped solar cells are depressed primarily by a reduction in bulk lifetime. Since the ingot impurity concentration remains to be determined, we cannot yet put the effects of tungsten in context relative to the severity of the effects compared to other impurities.

The situation for the cobalt-doped solar cells appears quite different from that of tungsten. Here the uncoated cell efficiencies vary from wafer to wafer over a range from about 5.8 to 8.6% with an average around 8% (85% of baseline), Table 10. There is considerable

TABLE 9

81201 W145W001 MAX CONCENTRATION W097 00 000
SOL11 12/18/78 AM1: PO=91.60MW/CM12 NO AR COATING

ID	ISC	VOC	IP	LOG(IO)	N	R	FF	FFF	OCD	PCDA	PCDB
2F*	21.90	.559	19.83	-6.532	1.92	-.89	.744	9.63	.00	.00	.00
1B	22.10	.553	20.51	-8.505	1.35	.17	.767	9.92	5.20	.00	.00
2B	22.10	.558	19.91	-6.275	2.02	-1.02	.738	9.62	4.16	.00	.00
3B	22.10	.557	19.91	-6.267	2.02	-1.02	.738	9.60	5.20	.00	.00
4B	22.10	.558	19.88	-6.217	2.04	-1.00	.735	9.58	4.81	.00	.00
5B	22.00	.558	19.82	-6.287	2.01	-.98	.737	9.57	3.90	.00	.00
1C	21.10	.536	19.03	-6.460	1.87	-.64	.732	8.76	1.69	.00	.00
2C	21.00	.537	18.01	-5.821	2.16	2.43	.612	7.30	1.56	.00	.00
3C	21.40	.531	18.55	-5.026	2.64	-1.47	.685	8.23	1.04	.00	.00
4C	21.10	.539	19.23	-7.056	1.67	-.33	.744	8.94	1.82	.00	.00
5C	21.20	.539	19.34	-7.315	1.60	.14	.737	8.90	2.21	.00	.00
6C	21.00	.534	18.73	-5.910	2.11	-1.04	.721	8.55	1.69	.00	.00
7C	21.40	.535	18.63	-5.066	2.63	-1.73	.695	8.42	1.43	.00	.00
8C	21.10	.530	18.22	-4.885	2.76	-1.84	.686	8.11	1.04	.00	.00
9C	21.10	.541	19.28	-7.262	1.62	-.21	.747	9.01	2.34	.00	.00
10C	21.10	.541	19.16	-6.991	1.70	-.03	.732	8.84	2.21	.00	.00
1S*	17.20	.540	10.86	-11.275	.95	21.77	.326	3.20	1.95	.00	.00
2S	21.20	.538	18.94	-6.002	2.08	-.95	.723	8.72	1.95	.00	.00
3S	21.30	.539	19.23	-6.670	1.80	-.15	.725	8.80	2.34	.00	.00
4S	21.30	.539	19.28	-6.637	1.81	-.59	.738	8.96	2.34	.00	.00
5S	21.30	.538	19.07	-6.084	2.04	-.90	.725	8.79	2.21	.00	.00
6S	21.10	.536	18.75	-5.772	2.19	-1.14	.717	8.58	1.82	.00	.00
1T	21.00	.538	18.55	-5.930	2.11	.09	.687	8.21	1.82	.00	.00
2T	21.00	.537	18.96	-6.577	1.83	-.45	.730	8.71	2.21	.00	.00
3T	21.10	.537	18.96	-6.316	1.93	-.62	.726	8.70	2.34	.00	.00
4T	21.00	.536	18.89	-6.338	1.92	-.70	.729	8.68	2.34	.00	.00
5T	21.10	.536	19.10	-6.749	1.76	-.28	.732	8.75	1.95	.00	.00
6T	21.40	.538	19.38	-6.805	1.75	-.15	.730	8.89	2.34	.00	.00
AVERAGES: 81201 BASELINE W097 00 000											
	22.08	.557	20.01	-6.710	1.89	-.77	.743	9.66	4.65	.00	.00
STD	.04	.002	.26	.898	.27	.47	.012	.13	.54	*	*
81201 W145W001 MAX CONCENTRATION											
	21.16	.537	18.92	-6.270	2.00	-.50	.717	8.61	1.94	.00	.00
STD	.14	.003	.36	.686	.33	.86	.029	.38	.40	*	*
PERCENT OF BASELINE											
	95.8	96.4	94.6	106.6	106	134.7	96.5	89.2	41.6	*****	*****
STD%	.8	.8	3.0	24.1	35	219.3	5.6	5.2	14.5	*****	*****

Table 9. Solar Cell I-V Data for a 4Ωcm p-type ingot doped with tungsten.

TABLE 10

81204 W146C0001 MAX CONCENTRATION W117 00 000
SOL11 12/26/78 AM1: PO=91.60MW/CM+2 NO AR COATING

ID	ISC	VOC	IP	LOG(IO)	N	P	FF	FFF	OCD	PCDA	PCDB
2B*	21.90	.556	19.64	-6.031	2.12	-1.25	.734	9.45	.00	.00	.00
1B	22.00	.552	20.21	-7.563	1.56	-.17	.755	9.69	5.20	.00	.00
2B	21.90	.549	19.94	-6.978	1.72	-.39	.744	9.46	4.55	.00	.00
3B.*	22.10	.549	19.75	-5.979	2.12	-.98	.724	9.29	4.16	.00	.00
4B	22.30	.551	20.26	-6.874	1.76	-.34	.739	9.61	4.94	.00	.00
5B	22.60	.550	20.66	-7.254	1.64	-.23	.748	9.83	5.20	.00	.00
1C	20.60	.530	17.83	-5.052	2.63	-1.30	.679	7.85	1.30	.00	.00
2C	20.50	.528	18.34	-6.253	1.93	-.32	.713	8.16	1.60	.00	.00
3C	20.90	.527	17.81	-4.668	2.95	-1.72	.665	7.74	1.17	.00	.00
4C.*	22.00	.540	17.71	-3.550	4.75	-4.87	.633	7.95	2.34	.00	.00
5C	21.00	.531	18.25	-5.227	2.50	-.88	.679	8.01	1.69	.00	.00
6C	21.90	.541	18.33	-4.178	3.59	-2.90	.658	8.24	2.60	.00	.00
7C	21.40	.540	19.19	-6.272	1.96	-.48	.720	8.80	2.60	.00	.00
8C.*	21.90	.536	16.08	-2.769	7.84	-9.22	.567	7.04	1.56	.00	.00
9C	20.80	.531	17.48	-4.261	3.44	-2.96	.663	7.74	1.43	.00	.00
10C.*	18.40	.501	14.34	-3.383	5.05	-5.59	.596	5.81	.33	.00	.00
11C.*	21.50	.538	17.85	-3.922	3.98	-4.29	.665	8.13	2.34	.00	.00
1S.*	21.60	.538	17.70	-3.785	4.23	-4.22	.646	7.94	2.08	.00	.00
2S.*	21.90	.543	18.00	-3.855	4.13	-3.82	.646	8.12	2.60	.00	.00
3S.*	21.90	.543	17.74	-3.558	4.76	-5.39	.646	8.12	3.00	.00	.00
4S.*	22.20	.541	17.63	-3.306	5.44	-6.44	.633	8.04	2.34	.00	.00
5S	21.80	.538	18.73	-4.730	2.93	-2.04	.682	8.46	2.60	.00	.00
1T.*	19.40	.514	15.16	-3.358	5.19	-5.69	.601	6.34	.52	.00	.00
2T.*	19.50	.508	14.28	-3.095	6.05	-4.53	.527	5.52	.26	.00	.00
3T	21.20	.536	18.76	-5.756	2.19	-.66	.702	8.43	2.47	.00	.00
4T.*	21.60	.533	16.60	-3.126	6.04	-6.57	.595	7.24	1.30	.00	.00
5T	21.50	.537	19.13	-5.984	2.08	-.50	.708	8.65	2.60	.00	.00
6T	21.00	.531	18.06	-4.864	2.78	-1.55	.675	7.96	1.69	.00	.00
AVERAGES: 81204 BASELINE W117 00 000											
	22.20	.551	20.27	-7.167	1.67	-.28	.747	9.65	4.97	.00	.00
STD	.27	.001	.26	.267	.08	.09	.006	.14	.27	*	*
81204 W146C0001 MAX CONCENTRATION											
	21.15	.534	18.36	-5.204	2.63	-1.39	.686	8.19	1.98	.00	.00
STD	.44	.005	.53	.723	.54	.90	.021	.35	.56	*	*
PERCENT OF BASELINE											
	95.2	96.9	90.6	127.4	158	*****	91.9	84.8	39.8	*****	*****
STD%	3.2	1.0	3.8	13.2	41	575.6	3.5	4.8	14.1	*****	*****

Table 10. Solar Cell I-V Data for a 4Ωcm p-type silicon ingot doped with cobalt.

evidence of junction degradation in the cobalt-bearing wafers; the baseline wafers appear free of this effect. Again, without concentration data it is difficult to put the magnitude of the cell degradation in perspective relative to the other impurities. However, the indication of junction degradation and possibly lifetime reduction in the cobalt doped cells is somewhat reminiscent of the behavior observed when iron and nickel (neighbors to cobalt in the periodic table) were introduced into silicon solar cells[1,2].

We expect to analyze the behavior of cobalt and tungsten in greater detail as more ingots and better concentration data become available.

3.4 Investigation of Anisotropy Effects in p-base Silicon Solar Cells

Once manufactured, a solar grade silicon feedstock will be processed via some crystal growth technique to wafers or sheet. We do not know whether radial or axial anisotropic impurity distributions introduced during the growth of the crystals will produce cell performance reductions over those which might be expected for uniformly doped wafers. Thus, a small portion of this program is directed at the evaluation of commercial size Czochralski-ingots and wide silicon webs grown from melts containing controlled amounts of contaminants. The first results from 3-inch diameter Czochralski ingots are reported below. In a parallel study we have also developed a first order model for the performance of solar cells which contain non-uniformities due to the variation in impurities, defects, etc. across the device.

3.4.1 Evaluation of 3-inch diameter Ti and Mn-doped Ingots

Two three-inch diameter ingots, W131, Mn 008 ($5.5 \times 10^{14} cm^{-3}$ Mn) and W140 Ti011 ($1.8 \times 10^{14} cm^{-3}$ Ti) were evaluated. Each process run consisted of 7 large wafers taken from seed, center and tang eng of the ingot. 1 cm x 1 cm miniature solar cells were fabricated on 5 large wafers by the standard process [1]. Thirty mil diameter mesa diodes were made on the remaining two wafers. Cell efficiency and OCD lifetime were measured on each miniature cell to map any anisotropy in ingot characteristics. The results of these experiments are summarized in

Tables 11 and 12. The first digit in the ID column of the tables represents the wafer number and the following digits desgnate the miniature cell number. Thus, an ID number of 112 implies the data are from the twelfth miniature cell of the first large wafer. The location of each miniature cell (1 to 12) is shown in Fig. 3. Figures 4 and 5 show the variation in the cell performance and the carrier lifetime of the miniature cells fabricated on a few of the large Mn and Ti doped wafers. Figure 6 shows the OCD lifetime map on a large Mn-doped crystal obtained by means of the 30 mil diameter mesa diodes. Work is in progress to obtain a similar lifetime map for Ti doped crystal. Apart from estimating the anisotropy due to the sedondary metal impurity, an attempt also was made to see the variation in the electrically active, primary dopant, boron. Resistivity was measured at various locations on the large wafer by the four point probe method and the results are shown in Fig. 7.

The data in Table 11 indicate that Mn incorporation in 3" diameter Czochralski crystals does not result in any striking anisotropy of the electrical characteristics. The average cell efficiency due to $5.5 \times 10^{14} cm^{-3}$ Mn in the large crystal was approximately 83% of the value for the uncontaminated baseline material. The maximum variation in the miniature cell performance across a wafer was $\pm$ 5%, and the variation over the entire ingot, irrespective of seed, center on the tang end, was within $\pm$ 10%. As expected from the cell performance, the OCD lifetime variation was also within the accuracy of the measurement technique (about a factor of 2). The average miniature cell efficiency was in very good agreement with the average cell performance on 1" diameter ingot-093 (about 86% of the baseline) containing comparable amount of Mn. Thus, the growth of large ingot has no appreciable influence on the incorporation of and the detrimental affect of the impurity. Our previous work established that Mn degrades the cell performance primarily by lowering the bulk lifetime; therefore, it is reasonable to say that impurity distribution is fairly uniform on 3" diameter Mn doped crystal.

TABLE 11

84026 W131MN008 (5.5E14) THREE INCH MATERIAL W117 00 000
SOL10 12/8 /78 AM1: PO=91.60MW/CM:2 NO AR COATING

ID	ISC	VOC	IP	LOG(IO)	N	F	FF	EFF	OCD	PCDA	PCDB
2B*	21.90	.560	19.74	-6.290	2.02	-1.02	.738	9.57	.00	.00	.00
11B	21.90	.555	20.12	-7.704	1.53	.13	.749	9.63	4.29	.00	.00
12B	22.20	.555	20.53	-8.169	1.42	.12	.761	9.92	3.90	.00	.00
13B.*	22.20	.552	19.82	-5.940	2.15	-.96	.722	9.35	3.64	.00	.00
14B	22.30	.556	20.70	-8.521	1.35	.21	.766	10.05	4.55	.00	.00
21B	22.30	.556	20.74	-8.664	1.32	.19	.770	10.10	4.03	.00	.00
22B	22.30	.556	20.74	-8.664	1.32	.19	.770	10.10	4.55	.00	.00
23B	22.30	.556	20.61	-8.084	1.44	.04	.762	9.99	4.94	.00	.00
24B	22.30	.556	20.65	-8.209	1.42	.02	.766	10.04	5.20	.00	.00
31B.*	22.10	.560	20.05	-6.313	2.01	-1.84	.766	10.03	3.00	.00	.00
32B	22.30	.560	20.39	-7.334	1.65	-.06	.745	9.83	4.94	.00	.00
33B	22.30	.560	20.61	-8.049	1.46	-.07	.765	10.10	5.20	.00	.00
34B	22.30	.558	20.18	-6.670	1.86	-.38	.733	9.65	4.68	.00	.00
41B	22.30	.558	20.65	-8.233	1.42	.02	.766	10.08	4.68	.00	.00
42B	22.60	.555	20.78	-7.673	1.54	-.07	.755	10.02	4.29	.00	.00
11	20.60	.527	17.65	-4.800	2.83	-1.57	.670	7.69	1.56	.00	.00
12	20.70	.534	18.45	-5.910	2.11	-1.01	.719	8.41	1.56	.00	.00
13	20.40	.536	18.32	-6.331	1.93	-.55	.723	8.36	.78	.00	.00
14	20.40	.525	17.30	-4.551	3.06	-2.03	.662	7.50	.46	.00	.00
15	20.30	.539	18.53	-7.122	1.66	-.50	.750	8.68	1.30	.00	.00
16	20.30	.534	17.84	-5.512	2.34	-.99	.697	7.99	.78	.00	.00
17	20.40	.537	18.28	-6.099	2.03	-1.04	.728	8.43	.91	.00	.00
18	20.30	.539	18.48	-6.920	1.72	-.64	.748	8.65	1.30	.00	.00
19	20.30	.538	18.40	-6.704	1.79	-.64	.740	8.55	1.30	.00	.00
110	19.80	.536	17.77	-6.146	2.02	-1.16	.732	8.22	1.04	.00	.00
111.*	19.40	.536	16.10	-3.767	4.35	-6.73	.688	7.56	1.30	.00	.00
21	20.60	.535	18.13	-5.433	2.38	-1.39	.705	8.29	1.04	.00	.00
22	20.60	.531	17.93	-5.271	2.47	-.91	.682	7.89	.91	.00	.00
23	21.10	.532	18.34	-5.078	2.61	-1.56	.690	8.20	.91	.00	.00
24	20.80	.536	18.44	-5.741	2.21	-1.02	.711	8.38	1.04	.00	.00
25	20.50	.533	17.81	-5.148	2.57	-1.31	.685	7.92	.91	.00	.00
26	20.50	.538	18.40	-6.273	1.96	-.70	.725	8.46	1.56	.00	.00
27	20.50	.537	18.31	-6.002	2.08	-1.02	.723	8.42	1.30	.00	.00
28	20.50	.539	18.55	-6.619	1.83	-.64	.737	8.62	1.56	.00	.00
29	20.50	.536	18.12	-5.585	2.30	-1.33	.711	8.27	1.30	.00	.00
210	20.40	.537	18.25	-6.056	2.05	-1.01	.725	8.40	1.30	.00	.00
211	19.90	.536	17.79	-6.038	2.06	-1.01	.723	8.16	1.17	.00	.00
212	19.80	.535	17.63	-5.830	2.17	-1.35	.723	8.10	1.56	.00	.00
31	20.50	.534	17.82	-5.155	2.57	-1.31	.686	7.94	.65	.00	.00
32	20.30	.537	18.09	-5.935	2.11	-.95	.717	8.27	.78	.00	.00
33	20.70	.531	17.63	-4.701	2.94	-1.53	.661	7.68	.65	.00	.00
34	20.60	.535	18.18	-5.602	2.28	-1.03	.704	8.20	1.04	.00	.00
35	20.40	.537	18.09	-5.762	2.20	-1.02	.711	8.24	1.04	.00	.00
36	20.70	.539	18.50	-6.060	2.06	-.83	.720	8.50	1.43	.00	.00
37	20.50	.535	17.93	-5.260	2.50	-1.53	.699	8.10	.91	.00	.00
38	20.70	.536	18.11	-5.318	2.46	-1.22	.694	8.14	1.04	.00	.00
39	20.50	.535	18.17	-5.700	2.23	-1.18	.713	8.27	1.04	.00	.00
310	20.80	.538	18.70	-6.291	1.95	-.79	.730	8.63	1.56	.00	.00
311	20.10	.534	17.75	-5.608	2.28	-1.17	.707	8.03	1.17	.00	.00
312	19.70	.527	17.01	-4.910	2.75	-1.96	.685	7.52	.91	.00	.00
41	20.40	.540	18.48	-6.703	1.80	-.54	.737	8.59	1.43	.00	.00
42	20.70	.540	18.75	-6.747	1.78	-.41	.735	8.69	1.69	.00	.00
43	20.80	.541	18.74	-6.413	1.91	-.71	.739	8.71	1.69	.00	.00
44	20.80	.540	18.88	-6.834	1.75	-.39	.738	8.76	1.69	.00	.00
45.*	20.90	.540	17.07	-2.854	7.50	*****	.816	9.74	1.95	.00	.00
46.*	21.00	.540	17.06	-2.805	7.79	*****	.811	9.72	1.95	.00	.00
47	20.70	.538	18.61	-6.293	1.95	-.83	.731	8.60	1.56	.00	.00
48	20.80	.534	18.31	-5.531	2.32	-1.02	.700	8.23	1.04	.00	.00
49	20.50	.535	18.36	-6.199	1.98	-.67	.721	8.37	1.30	.00	.00
410	20.60	.532	18.25	-5.670	2.23	-1.22	.713	8.27	1.04	.00	.00
411	20.20	.534	18.17	-6.325	1.93	-.81	.730	8.33	1.56	.00	.00
412	20.00	.535	17.85	-5.994	2.08	-1.00	.721	8.16	1.56	.00	.00
51	20.60	.536	18.04	-5.321	2.46	-1.35	.697	8.14	1.04	.00	.00
52	20.50	.536	18.30	-6.020	2.07	-.87	.719	8.36	1.04	.00	.00
53	20.50	.538	18.15	-5.686	2.25	-1.10	.710	8.28	1.04	.00	.00
54	20.50	.538	18.41	-6.306	1.95	-.60	.724	8.44	1.04	.00	.00
55	20.40	.537	18.39	-6.478	1.87	-.55	.729	8.45	1.30	.00	.00
56	20.50	.534	18.14	-5.705	2.22	-.95	.706	8.18	.91	.00	.00
57	20.60	.537	18.57	-6.538	1.85	-.36	.726	8.49	1.43	.00	.00
58	20.50	.537	18.57	-6.776	1.76	-.36	.734	8.55	1.17	.00	.00
59	20.30	.535	18.26	-6.552	1.84	-.07	.717	8.24	1.30	.00	.00
510	20.20	.535	18.13	-6.247	1.96	-.74	.725	8.29	1.17	.00	.00
511	19.80	.534	17.87	-6.599	1.82	-.39	.728	8.14	.91	.00	.00
512	19.70	.533	17.79	-6.716	1.78	-.17	.725	8.05	1.17	.00	.00
AVERAGES: 81026 BASELINE W117 00 000											
	22.28	.557	20.56	-7.998	1.48	.03	.759	9.96	4.60	.00	.00
STD	.15	.002	.21	.555	.15	.16	.011	.16	.41	*	*

Table 11. Miniature solar cell parameters and OCD lifetimes on 3 in diameter Mn-doped wafers.

TABLE 12a

81031 W140T1011 (1.5E14) THREE INCH MATERIAL [illegible] 00 000
SOL10 12/1 /78 AM1: PO=91.60MW/CM^2 NO AR COATING

ID	ISC	VOC	IP	LOG(IO)	N	R	FF	EFF	OCT	PCDA	PCDF
2R*	21.90	.555	19.71	-6.213	2.04	-1.12	.738	9.49	.00	.00	.00
11B	22.80	.553	21.07	-8.153	1.42	.18	.759	10.12	5.20	.00	.00
12B.*	22.30	.546	19.46	-5.145	2.61	-1.51	.696	8.96	2.60	.00	.00
13B	22.20	.551	20.42	-7.672	1.53	-.15	.757	9.80	5.85	.00	.00
14B	22.30	.551	20.46	-7.471	1.58	-.22	.754	9.80	5.60	.00	.00
21B.*	22.40	.548	19.89	-5.751	2.23	-.98	.714	9.27	3.64	.00	.00
22B.*	22.60	.546	19.54	-4.878	2.82	-1.78	.687	8.97	3.00	.00	.00
23B	22.30	.553	20.43	-7.392	1.61	-.20	.751	9.80	3.90	.00	.00
24B	22.10	.553	20.35	-7.801	1.50	-.05	.757	9.79	3.90	.00	.00
31B	22.00	.550	20.27	-7.816	1.49	-.05	.758	9.70	3.64	.00	.00
32B	22.00	.550	20.21	-7.682	1.53	.10	.749	9.59	1.56	.00	.00
33B	22.20	.551	20.31	-7.310	1.63	-.19	.748	9.68	4.55	.00	.00
34B	22.40	.550	20.54	-7.440	1.59	-.21	.753	9.81	4.55	.00	.00
41B	22.00	.553	20.12	-7.308	1.63	-.15	.746	9.60	3.64	.00	.00
42B	22.20	.553	20.50	-8.081	1.44	.13	.759	9.85	4.42	.00	.00
43B	22.10	.555	20.47	-8.332	1.39	.20	.762	9.89	4.68	.00	.00
44B	22.10	.555	20.50	-8.455	1.36	.18	.766	9.94	4.68	.00	.00
51B	22.20	.553	20.62	-8.541	1.34	.17	.768	9.97	5.20	.00	.00
52B	21.90	.556	20.20	-7.877	1.49	-.15	.762	9.82	4.31	.00	.00
11	12.50	.479	11.34	-7.444	1.44	.95	.718	4.55	.91	.00	.00
12	12.50	.477	11.30	-7.154	1.52	.58	.716	4.52	.91	.00	.00
13	12.60	.477	11.37	-7.058	1.54	.56	.714	4.54	.91	.00	.00
14	12.50	.476	11.30	-7.143	1.52	.58	.716	4.51	.91	.00	.00
15	12.60	.476	11.37	-7.047	1.54	.56	.713	4.52	.91	.00	.00
16	12.60	.473	11.30	-6.734	1.63	.39	.705	4.45	.91	.00	.00
17	12.60	.476	11.40	-7.240	1.49	.74	.716	4.54	1.04	.00	.00
18	12.60	.476	11.37	-7.047	1.54	.56	.713	4.52	1.04	.00	.00
19	12.50	.475	11.27	-7.024	1.55	.60	.711	4.47	1.17	.00	.00
110	12.50	.477	11.27	-7.045	1.55	.60	.712	4.49	.91	.00	.00
111	12.10	.475	10.93	-7.191	1.50	.84	.712	4.33	1.04	.00	.00
112	12.10	.477	10.91	-7.071	1.55	.69	.711	4.34	.91	.00	.00
21	12.20	.468	10.77	-6.151	1.85	.25	.684	4.13	.91	.00	.00
22	12.30	.474	10.98	-6.554	1.70	.31	.700	4.32	.91	.00	.00
23	12.30	.474	10.95	-6.477	1.73	.34	.696	4.29	.91	.00	.00
24	12.10	.474	10.97	-7.425	1.44	.94	.717	4.35	.91	.00	.00
25	12.30	.474	11.11	-7.167	1.51	.73	.714	4.40	.91	.00	.00
26	12.10	.474	10.97	-7.425	1.44	.94	.717	4.35	1.04	.00	.00
27	12.30	.474	11.11	-7.167	1.51	.73	.714	4.40	1.04	.00	.00
28	12.30	.473	11.08	-6.996	1.55	.57	.711	4.38	.91	.00	.00
29	12.20	.472	11.02	-7.089	1.52	.47	.716	4.36	1.04	.00	.00
210	12.00	.472	10.89	-7.470	1.42	.93	.719	4.31	1.04	.00	.00
211	11.90	.471	10.78	-7.342	1.45	.87	.716	4.25	.91	.00	.00
212	11.90	.471	10.78	-7.342	1.45	.87	.716	4.25	1.04	.00	.00

Table 12. Miniature solar cell parameters and OCD lifetimes on 3 in diameter T-doped wafers.

TABLE 12b

31	12.70	.480	11.46	-7.039	1.54	.75	.711	4.58	.91	.00	.00
32	12.80	.478	11.53	-7.010	1.56	.77	.708	4.58	.91	.00	.00
33	12.60	.478	11.45	-7.557	1.41	1.12	.717	4.57	.91	.00	.00
34	12.50	.475	11.27	-7.024	1.55	.60	.711	4.47	.91	.00	.00
35	12.60	.479	11.35	-7.040	1.56	.77	.708	4.52	.78	.00	.00
36	12.80	.480	11.49	-6.764	1.65	.37	.707	4.60	.91	.00	.00
37	12.70	.478	11.37	-6.637	1.68	.18	.706	4.54	.91	.00	.00
38	12.50	.475	11.21	-6.758	1.63	.45	.705	4.43	1.04	.00	.00
39	12.60	.476	11.33	-6.868	1.60	.38	.711	4.51	1.04	.00	.00
310	12.80	.478	11.51	-6.856	1.61	.36	.711	4.60	.91	.00	.00
311	12.50	.477	11.24	-6.812	1.62	.23	.712	4.49	1.04	.00	.00
312	12.50	.475	11.21	-6.758	1.63	.45	.705	4.43	.78	.00	.00
41	12.00	.470	10.87	-7.356	1.44	.97	.714	4.26	.78	.00	.00
42	12.00	.470	10.82	-7.184	1.49	1.06	.707	4.22	.78	.00	.00
43	12.10	.472	10.87	-6.833	1.60	.36	.709	4.28	1.04	.00	.00
44	12.10	.471	10.92	-7.091	1.52	.65	.712	4.29	.91	.00	.00
45	12.10	.471	10.78	-6.445	1.74	.15	.698	4.21	.78	.00	.00
46	12.00	.471	10.84	-7.171	1.50	.65	.715	4.27	.91	.00	.00
47	12.00	.471	10.82	-7.089	1.52	.70	.712	4.25	.91	.00	.00
48	12.00	.471	10.87	-7.367	1.44	.97	.715	4.27	.91	.00	.00
49	12.00	.469	10.86	-7.232	1.47	.61	.718	4.27	1.04	.00	.00
410	11.90	.469	10.77	-7.319	1.45	.87	.716	4.22	.91	.00	.00
411	11.60	.471	10.47	-7.055	1.54	.42	.716	4.14	.91	.00	.00
412	11.40	.469	10.07	-5.965	1.95	-1.24	.702	3.97	1.04	.00	.00
51	12.10	.478	10.94	-7.224	1.50	.84	.713	4.36	.91	.00	.00
52	12.20	.475	11.01	-7.149	1.52	.87	.710	4.35	1.04	.00	.00
53	12.00	.469	10.62	-6.210	1.83	.00	.691	4.11	.65	.00	.00
54	12.10	.474	10.97	-7.363	1.45	.76	.719	4.36	1.04	.00	.00
55	12.10	.476	10.98	-7.512	1.42	1.13	.716	4.36	2.60	.00	.00
56	11.90	.474	10.83	-7.604	1.39	.95	.723	4.31	.91	.00	.00
57	12.20	.473	11.00	-7.010	1.55	.50	.713	4.35	.91	.00	.00
58	12.30	.473	11.08	-6.996	1.55	.57	.711	4.38	.91	.00	.00
59	12.10	.473	10.97	-7.352	1.45	.76	.719	4.35	.78	.00	.00
510	12.00	.469	10.73	-6.677	1.65	.51	.700	4.17	.78	.00	.00
511	11.80	.470	10.70	-7.517	1.40	1.34	.712	4.18	.78	.00	.00
512	11.80	.469	10.52	-6.451	1.73	-.11	.704	4.12	.78	.00	.00
AVERAGES:	81031 BASELINE W097 00 000										
	22.19	.552	20.43	-7.822	1.50	-.03	.757	9.81	4.41	.00	.00
STD	.21	.002	.22	.398	.09	.16	.006	.13	1.00	*	*
	81031 W140TI011 (1.8E14) THREE INCH MATERIAL										
	12.25	.474	11.04	-7.036	1.55	.60	.711	4.37	.95	.00	.00
STD	.31	.003	.29	.348	.11	.37	.007	.14	.23	*	*
PERCENT OF BASELINE											
	55.2	85.8	54.0	110.1	103	*****	94.0	44.5	21.6	*****	*****
STD%	1.9	.8	2.0	9.3	14	*****	1.7	2.1	11.4	*****	*****

Dwg. 7684A13

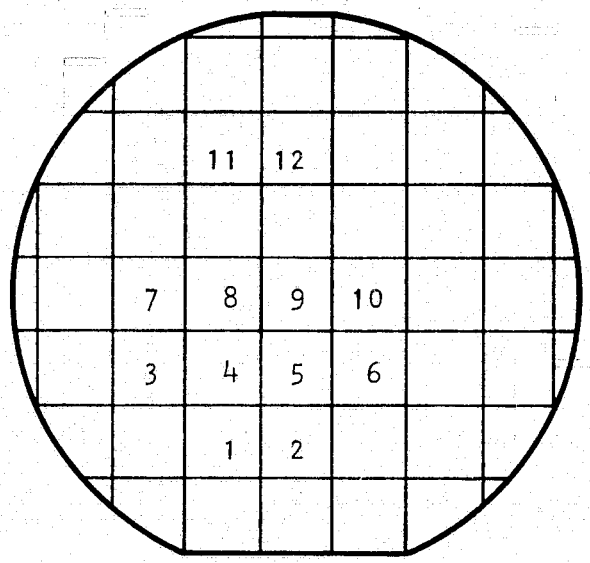

Figure 3. Location of miniature cells on large wafer.

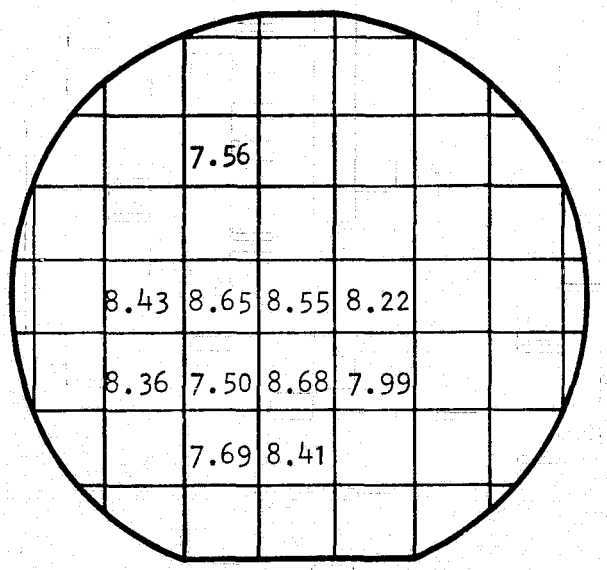

(a)

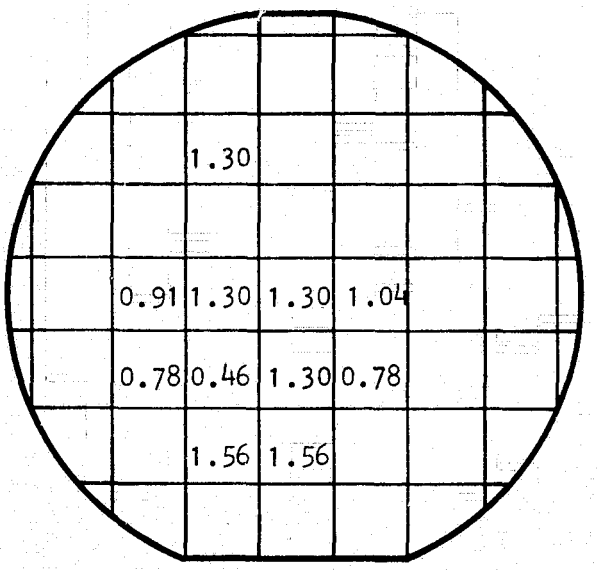

(b)

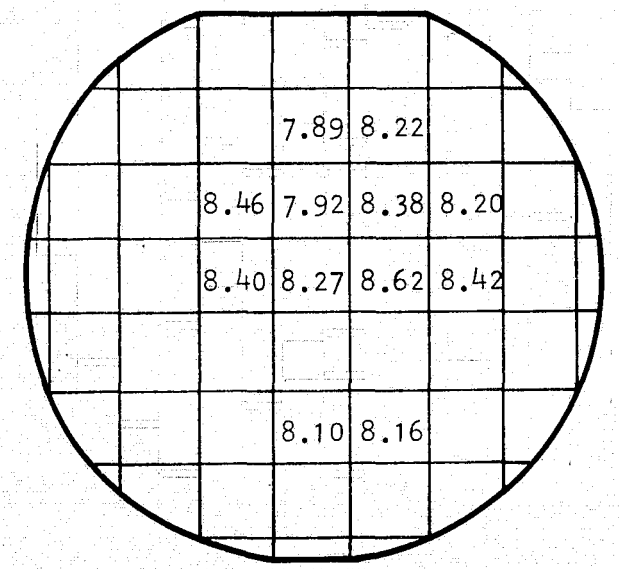

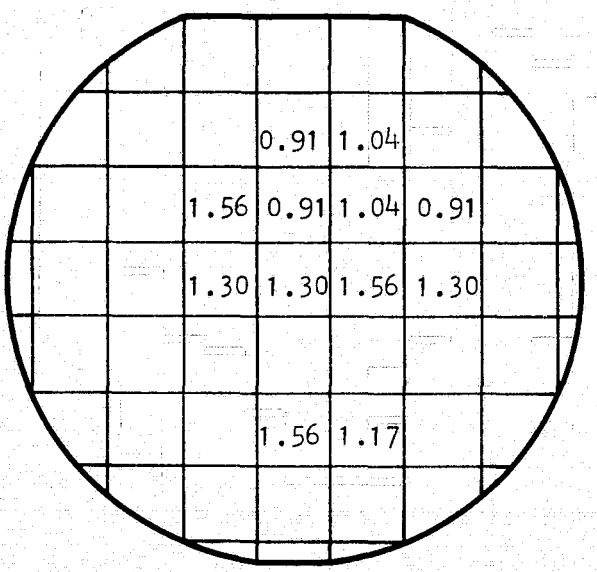

Figure 4. (a) Cell efficiencies (%) and (b) Corresponding OCD lifetimes (μsec) for miniature solar cells distributed across 3 inch diameter Mn-doped CZ wafers.

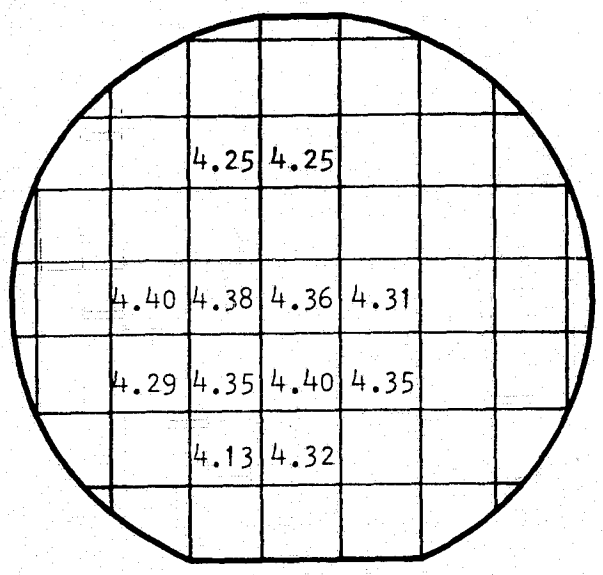

(a)

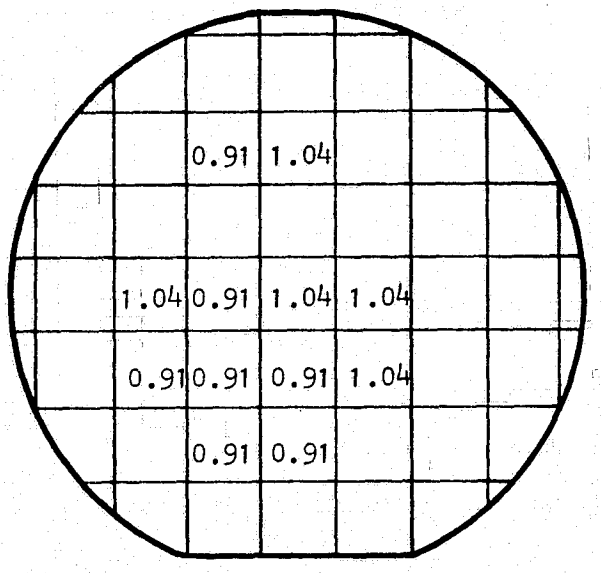

(b)

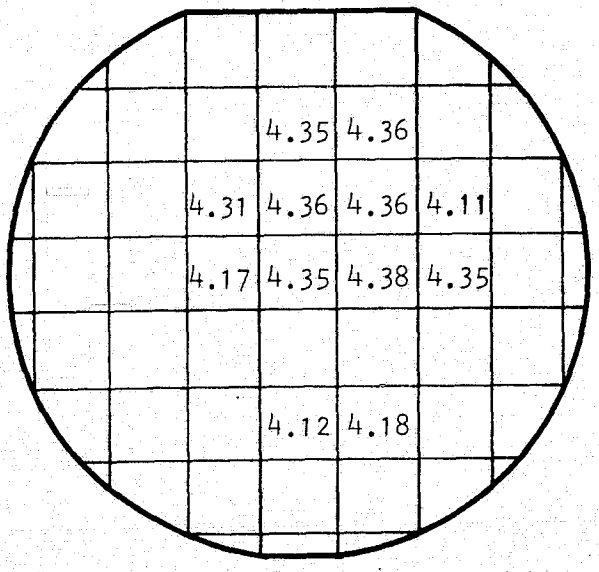

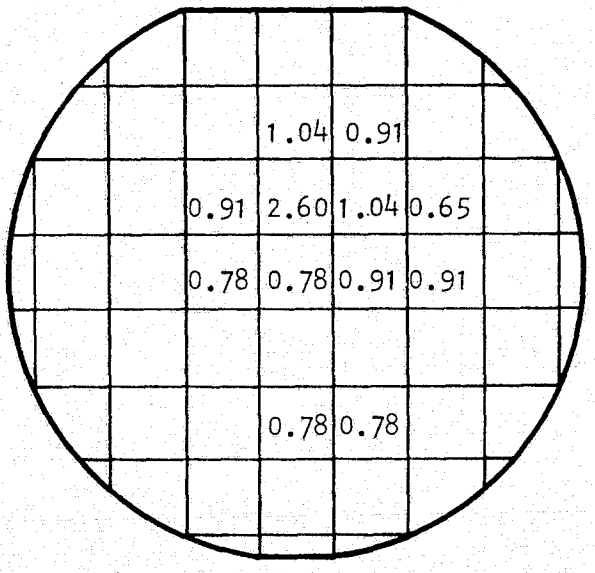

Figure 5. (a) Cell efficiencies (%) and (b) corresponding OCD lifetimes (μsec) for miniature solar cells distributed across 3 inch diameter Ti-doped CZ wafers.

Dwg. 7684A12

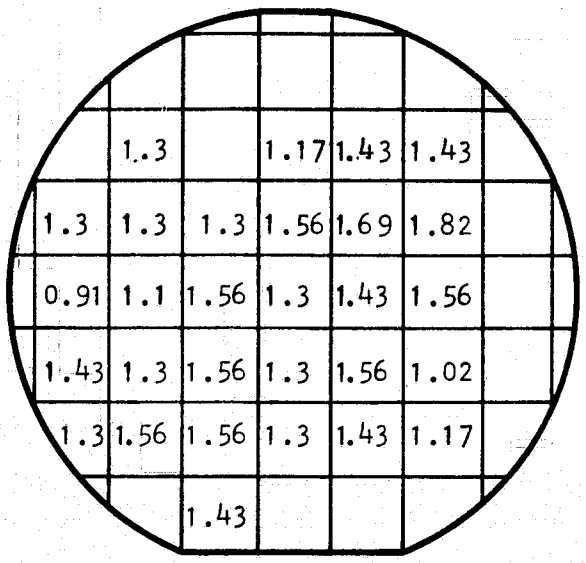

Figure 6. OCD lifetimes (μsec) measured on 30 mil diameter mesa diodes distributed across a 5 inch diameter Mn-doped CZ wafer.

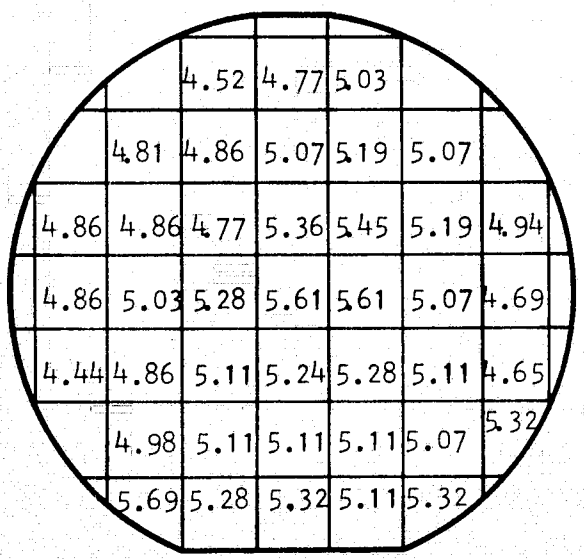

Figure 7. Resistivity Variation across a 3 inch diameter Mn-doped CZ wafer.

The results on ingot W-140-Ti-011, Table 12 and Fig. 5, also reveal no striking anisotropy due to Ti incorporation in the large crystal. The maximum variation in the miniature cell performance across any wafer was ± 5%, which is close to our experimental accuracy. Regardless of whether the wafers came from the seed, center or the tang end, the average miniature cell performance was ~ 4.37% of the baseline, with a scatter of less than ± 10%. The average efficiency is very close to the performance predicted by 1 cm x 1 cm cells made on 1" diameter ingot-123, which have comparable Ti content (1 x 10^{14} cm^{-3} Ti resulted in 52% of the baseline efficiency).

Thus, our studies so far, suggest that impurities like Mn and Ti, which reduce the cell performance primarily by lowering the bulk lifetime, are distributed fairly uniformly throughout the 3" diameter ingots. No striking anisotropy was detected. The variation in the miniature cell performance across a wafer was ± 5% and over the entire ingot (seed, center and tang) was ± 10%. The variation in OCD lifetime was within the experimental accuracy of the measurement-technique. The variation in the resistivity was also ± 10%. The affect of impurities, like Mn and Ti, was found to be similar on 1" and 3" diameter crystals.

3.4.2 Modeling the Behavior of Non-Uniform Devices

It would be fortuitous if impurities and defects were uniformly distributed in a real solar cell. But since they are not, it is informative to examine how uneven properties influence the performance of the cell.

For analysis a non-uniform cell can be considered as several parallel connected cells with differing areas and characteristics. Each of these sub-cells can be represented by the lumped equivalent circuit of Figure 8.

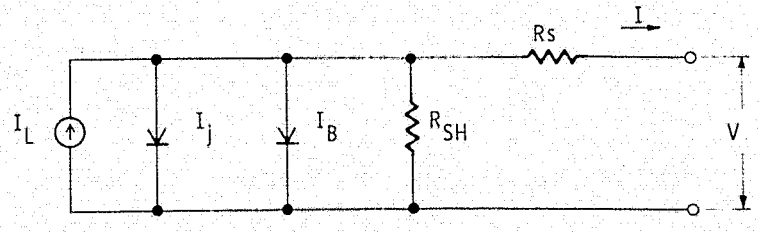

Figure 8.

Where I_L is the light generated current,
I_j is the junction recombination current,
I_B is the diffusion current
R_S and R_{SH} are the series and shunt resistances

Since the cell is a distributed device, these parameters are area dependent. In particular, the resistances are usually better described in terms of specific resistanc es, such that:

$$R_s = R_{sp}/A \qquad (1)$$

and

$$R_{sh} = R_{shp}/A \qquad (2)$$

In a typical good device, the specific series R_{sp} is about 0.3 ohm cm^2 and depends primarily on the contact grid design and the diffusion sheet resistance. In the specific shunt resistances, R_{shp} is typically greater than 50 kilohms and is a consequence of junction defects, e.g. precipitates, pipes, localized crystal defects and physical damage. In a case, where shunt conductance is large, it is likely to be highly non-uniform over the cell area. The remaining elements in Figure 8 are controlled by the carrier lifetime in the various regions of the cell, plus, as is observed in the case of I_L, by the illuminating spectrum. While I_L cannot be expressed in closed form for a real spectrum, a good approximation can be obtained by using an energy equivalent monochromatic illumination [1] and by assuming all the light is absorbed in the cell base.

$$I_L = \frac{A\ J_{LO}}{\frac{L_\lambda}{L_n} + 1} \qquad (3)$$

where J_{LO} = the maximum photo-current density
L_λ = the absorption length of the incident light
L_n = the base diffusion length

The junction and base currents for a diffusion length limited device are written as:

$$I_j = AJ_{02}\ \left(\exp\left(\frac{V + IR_s}{2\ V_T}\right) - 1\right) \qquad (4)$$

I = the terminal current

$$J_{02} = \frac{Wq\ D_n\ n_i}{2\ L^2_{nd}} \cong \frac{C_2}{L_{nd}}$$

C_2 = a constant

W = the depletion width

L_{nd} = the diffusion length in the depletion region

D_n = the diffusion const.

$$I_B = AJ_{01}\ (\exp\ \frac{V + IRs}{V_T} - 1$$

$$J_{01} = \frac{q\ n_i^2}{N_A\ L_{nb}} = \frac{C_1}{L_{nb}} \qquad (5)$$

N_A = base acceptor concentration

We can now write an expression for the terminal current - voltage behavior of a single device as a function of its diffusion length, area and the two specific resistances.

$$I = I_L - I_j - I_B - I_{R_{sh}} \qquad (6)$$

$$I = \frac{AJ_{LO}}{\frac{L_A}{L_{nb}} + 1} - \frac{C_2 A}{L_{nd}} \exp \frac{V + I\ R_{sp}/A}{2V_t} - 1$$

$$- \frac{C_1 A}{L_{nb}} \exp \frac{V + I\ R_{sp}/A}{V_t} - 1 - \frac{V + I\ R_{sp/A}}{R_{shp}/A} \qquad (7)$$

For the non-uniform device with several dissimilar areas functioning in parallel, the voltages for each sub-device are the same and the total current is simply the sum of the currents given by Equation 7 for each of sub-devices.

The peak power and efficiency are determined from:

$$\frac{dP}{dV} = I + V \frac{dI}{dV} = 0 \qquad (8)$$

obtaining I and $\frac{dI}{dV}$ from eq. 7. Eq. 8 is linear in V so that the composite device equation is a linear sum of the equations representing the sub-devices.

These equations enable characterization of the composite device in terms of the properties of its sub-regions and, therefore, allow the prediction of cell performance from data on the anisotropy of the crystal properties. Furthermore, as grain boundaries can be approximately characterized in terms of effective diffusion length, area and resistances, we can also model the behavior of polycrystalline devices. An illustrative case for a two region device is shown graphically in Figure 9. The IV curves are shown for the two sub-devices and the combined device.

Note that $I_3 = I_1 + I_2 \equiv I_1 - \left(-I_2\right)$.

By plotting $-I_2$ against voltage we obtain the total current, I_3 as the length of vertical vector drawn from I_2 to I_1 at any voltage. From this figure, it is apparent that V_{OC} of the total device occurs where $I_1 = -I_2$, that is, where I_1 crosses $-I_2$. One can also see that the poorer device, I_2, extracts energy from the better one for voltages above its open-circuit value.

Another view of anisotropy effects is shown in Fig. 10. The cell consists of two elements, one with an assumed efficiency of 15.5%, the other with an assumed efficiency of 4 %. The total cell performance is calculated with the relative area as a parameter for two cases. The lowest curve assumes the defective device has a fixed, area-independent shunt resistance of 100 ohms. The other curve assumes a specific shunt resistance of 100 ohms.

The broken line is a linear approximation obtained by simply adding the sub-cell power contributions, that is, assuming there is no interaction between the two sub-cells.

It is important to include the series resistance effects in these calculations since the distributed resistance acts as an area dependent decoupling resistance between good and bad regions of the device. This decoupling resistance increases as the defective area diminishes. Thus, the impact of a small region with low lifetime is less than would be predicted if the resistance were neglected.

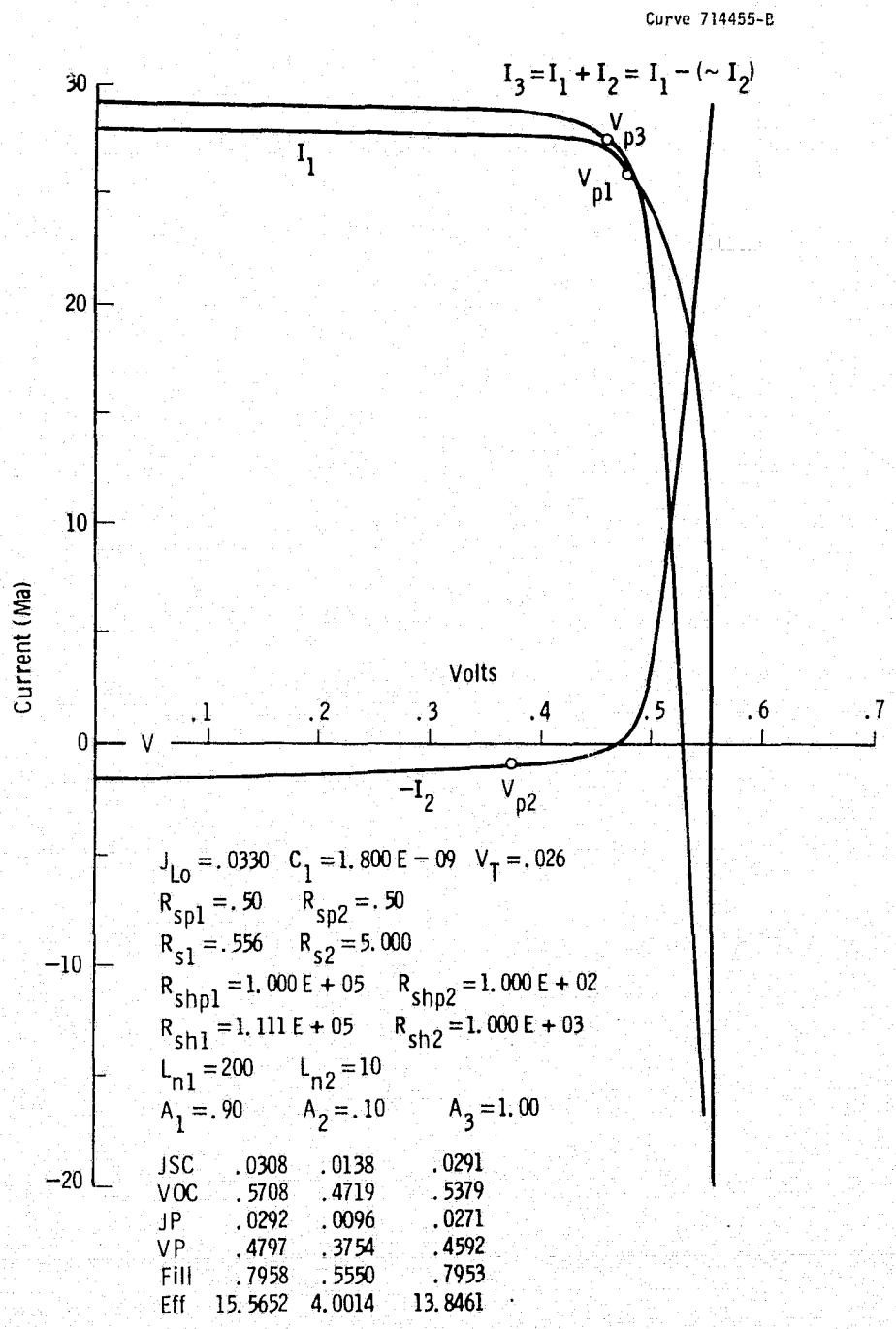

Figure 9. Calculated I-V curves for two regions of a solar cell with dissimilar properties. Shown also is the I-V curve for the composite cell. The current I_2 is plotted negatively so that the total current, $I_3 = I_1 + I_2$ is simply the vector drawn from I_2 to I_1.

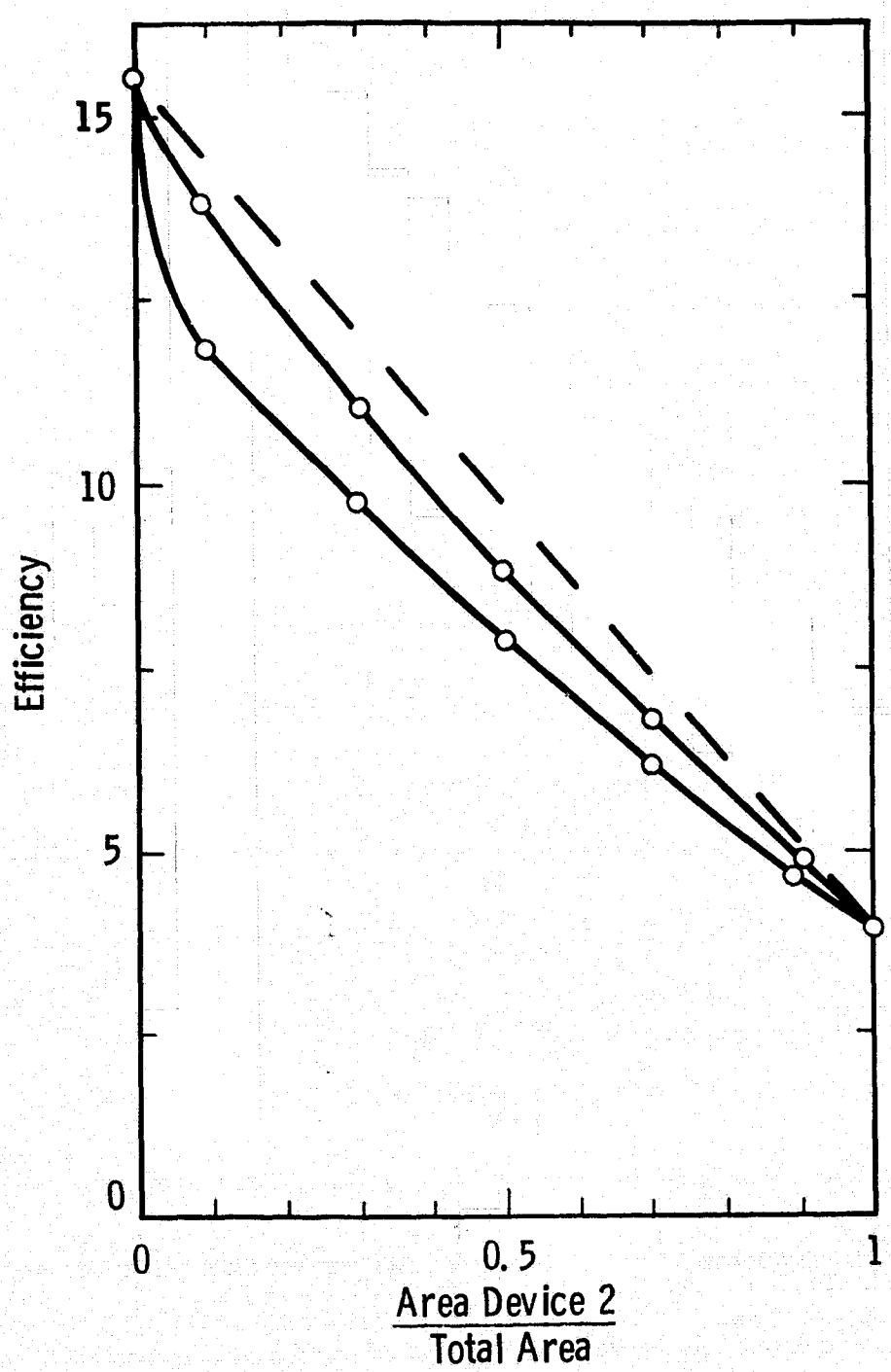

Figure 10. Calculated performance of a non-uniform device as a function of the relative area of the defective region. The lowest curve assumes constant shunt resistance. The middle curve assumes an area dependent shunt resistance. The dashed curve is a simple linear approximation assuming no interreaction between the two regions.

The degree of decoupling will depend in an unpredictable manner on the size and location of the defective area as a function of its placement relative to the contact grid.

This model analysis can be used to interpret the implications of the impurity anisotropy experiments which provide contour maps of lifetime and shunt resistance from which the sub-areas of the model can be defined.

Data for lifetime anisotropy in a manganese doped wafer is shown in Fig. 6 in section 3.4.1. These results are typical of recent studies and show so little non-uniformity that its effect can be neglected. The model calculation for this is indistinguishable from the linear approximation. It is generally apparent that the effects of anisotropy are small except in the case where the regional differences are very large.

3.5 Permanence of Impurity Effects in Silicon Solar Cells

Experimental evidence shows that solar cell performance is a function of device processing and that the degree of degradation due to specific impurities also varies with process history. Since the useful life of solar cells in the field must be many years, it is of some interest to determine how stable the performance of cells made on impure silicon will be over extended periods. That is, how permanent will be the characteristics of solar cells fabricated on solar grade silicon. We are conducting some preliminary studies to evaluate the importance of this question.

Two impurities which produce strong degradation in cell performance, Ti and Mo, were chosen for the first experiments. Wafers from ingots W123 Ti 008 ($1x10^{14}$Ti) and W077 Mo 001 ($4.2x10^{12}$ Mo), along with baseline ingot W097, are being processed according to the matrix depicted in Figure 3 of the 12th Quarterly report[4]. So far the solar cells have been made on wafers from each ingot in order to characterize the properties prior to temperature stressing. For example, data from

the baseline wafer are given in Table 13. Following the thermal stress experiments at the various times and temperatures shown in the matrix, the new performance data will be compared with the baseline values.

TABLE 13

SOLAR CELL PROPERTIES OF INGOTS FOR PERMANENCE STUDIES

	ID	ISC	VOC	IP	LOG(IO)	N	R	FF	EFF	OCD
BASELINE 097	2R*	21.90	.555	19.68	-6.125	2.08	-1.20	.737	9.47	.00
	9	21.90	.555	19.99	-7.059	1.72	-.51	.750	9.64	4.68
	10	21.80	.553	19.95	-7.250	1.65	-.41	.753	9.60	5.20
	11	22.00	.551	19.76	-6.174	2.04	-.95	.732	9.38	4.42
	12	21.80	.552	19.98	-7.372	1.61	-.34	.755	9.60	4.55
	13	22.10	.555	20.35	-7.686	1.54	-.25	.761	9.87	5.85
	14	22.00	.553	20.01	-6.843	1.78	-.60	.746	9.60	3.64
	15	22.00	.550	19.43	-5.508	2.39	-1.34	.711	9.10	3.64
W123-T1008	25	14.30	.482	12.75	-6.424	1.76	.21	.699	5.09	.65
	26	14.40	.482	12.86	-6.460	1.74	.07	.704	5.17	.65
	27	14.30	.483	12.76	-6.510	1.73	.40	.698	5.10	.65
	28	14.20	.481	12.62	-6.257	1.82	-.03	.697	5.04	.65
	29	14.30	.480	12.73	-6.332	1.79	.01	.700	5.08	.65
	30	14.40	.481	12.77	-6.143	1.87	-.25	.698	5.11	.65
	31	14.40	.478	12.76	-6.116	1.87	-.25	.696	5.07	.65
	32	14.30	.478	12.64	-6.184	1.84	.46	.683	4.93	.65
W0T1Mo-001	41	18.50	.502	16.43	-6.001	1.96	-.43	.703	6.90	.65
	42	18.90	.506	16.86	-6.065	1.95	-.72	.715	7.23	.65
	43	18.60	.505	16.48	-5.850	2.05	-.74	.705	7.00	.65
	44	18.40	.503	16.44	-6.198	1.88	-.53	.714	6.99	.55
	45	18.90	.503	16.75	-5.869	2.03	-.65	.704	7.07	.65
	46	18.60	.503	16.50	-5.816	2.06	-1.01	.711	7.03	.65
	47	18.50	.504	16.57	-6.277	1.85	-.59	.720	7.10	.65

4. CONCLUSIONS

The first detailed gettering experiments we conducted on Fe, Ti and Mo-doped ingots indicate that for Fe and Ti contaminants: (1) raising the temperature during $POCl_3$ gettering at constant time improves solar cell performance and (2) for fixed gettering temperature, extending the time also increases cell performance. The temperature and time ranges investigated were 950 to 1100°C and 1 to 5 hours. In contrast, virtually no improvement in solar cells made on Mo-doped wafers was gained by gettering treatments. Despite the fact that gettering improves the efficiency of contaminated devices, the benefits are small (absolute efficiency increases up to 1.5 percentage points since the devices require prolonged exposure to high temperature, at least for the impurity concentrations studied so far.

The commercial size (3 in diameter) Czochralski ingots doped with Mn or Ti were mapped via miniature solar cells and diodes in an attempt to discover any non-uniformities in electrical characteristics due to anisotropic impurity incorporation. No significant variation in cell performance or OCD lifetime either across a wafer or along the ingots could be found. The magnitudes of solar cell efficiencies measured on the large ingots were quite close to that found on small (1 in) diameter test ingots bearing similar amounts of impurity. Thus, at least for Ti and Mn non-uniform impurity distribution does not appear to degrade cell performance in larger ingots. Moreover, the small ingots predict well the impurity-cell performance behavior of the larger ingots.

The first generation W-doped ingot produced solar cells whose performance was degraded to about 89% of the baseline values. The reduction in cell efficiency is due primarily to a loss in bulk lifetime. In contrast, the first Co-doped ingot produced solar cells whose I-V parameters suggest that junction quality as well as bulk lifetime are degraded. This behavior is similar to that displayed by Cu and Fe-doped

cells, as might be guessed from the relative positions of each element in the periodic table. No conclusion can yet be drawn as to the relative effects of Co or W compared to other impurities since it has not been possible to chemically detect these impurities in the ingot yet.

5. PROGRAM STATUS

5.1 Present Status

The program plan for Phase III of this program is depicted in Figure 11. The program is generally on schedule. Work on the anisotropy studies was initiated ahead of plan.

- During this past quarter:
- Eleven ingots were prepared for subsequent chemical, electrical and cell evaluation.
- Spark source mass spectroscopy, microstructural evaluation, resistivity probing, and carbon/oxygen analysis were performed on all ingots grown.
- Gettering experiments at three temperatures (950°, 1000° and 1100°) and various times were completed on iron, titanium and molybdenum-bearing ingots.
- Evaluation of the first generation cobalt and tungsten-doped ingots was completed.
- An assessment was made of the uniformity of electrical characteristics and solar cell performance in commercial-size (3 inch diameter) Ti and Mn-doped ingots.
- A model was developed to predict the cell performance in non-uniform devices.
- Studies of permanence effects in Ti and Mo-doped ingots were initiated.

5.2 Future Activity

During the next quarter effort will be directed primarily into four areas: (1) thermochemical processing - continued evaluation of phosphorus gettering effects and HCℓ gettering (2) evaluation of second

and third generation n-base ingots, as well as multiply-doped ingots (3) modeling the behavior of n-base solar cells containing metal contaminants (4) assessment of permanence effects (thermal stressing) in Ti and Mo-doped solar cells.

6. REFERENCES

1. R. H. Hopkins, et al., 11th Quarterly Report and Summary, Silicon Materials Task (Part 2) DOE/JPL 954331-78/3, July 1978.

2. R. H. Hopkins, et al., 5th Quarterly Report and Summary, Silicon Materials Task (Part 2) DOE/JPL 954331-77/1, January 1977.

3. R. H. Hopkins, et al., 3rd Quarterly Report, Silicon Materials Task (Part 2) DOE/JPL 954331-76/3, July 1976.

4. R. H. Hopkins, et al., 12th Quarterly Report, Silicon Materials Task (Part 2) DOE/JPL 954331-78/4, October 1978.

7. Appendices

Appendix 7.1 Segregation Coefficients

Element	Segregation Coefficient
Al	3×10^{-2} (2.8×10^{-3})
B	0.8
C	0.05
Ca	?
Cu	8.0×10^{-4}
Cr	1.1×10^{-5}
Fe	6.4×10^{-6}
Mg	3.2×10^{-6}
Mn	1.3×10^{-5}
Mo	4.5×10^{-8}
Ni	3.2×10^{-5}
Ph	0.35
Ta	$\sim 10^{-7}$
Ti	2.0×10^{-6}
V	4×10^{-6}
Zn	10^{-5}
Zr	$< 1.6 \times 10^{-8}$
Co	$< 1.1 \times 10^{-5}$
W	$< 1.6 \times 10^{-6}$

Appendix 7.2 : Impurity Concentrations of Phase III ingots

Ingot Identification	Target Concentration 10^{15} atoms/cm^3	Calculated Concentration 10^{15} atoms/cm^3	Measured Concentration 10^{15} atoms/cm^3
W-129-00-000 (7.6 cm)	NA	NA	NA
W-130-00-000 (7.6 cm)	NA	NA	NA
W-131-Mn-008 (7.6 cm)	0.6	0.55	0.55
W-132-Ta-003	0.0002	0.0009	<0.5
W-133-00-000	NA	NA	NA
W-134-Ti-009	0.05	0.03	<0.25
W-135-Fe-005	1.0	0.78	<1.5
W-136-Fe-006	0.3	0.24	<1.5
W-137-Ti-010	0.2	0.2	<0.25
W-138-Mo-005	0.001	0.0008	<0.5
W-139-Mo-006	0.0042	0.0054	<0.5
W-140-Ti-011 (7.6 cm)	0.18	0.18	<0.25
W-141-Mo/Cu-001	0.004/4.42	0.003/3.68	<0.5/4.00
W*-142-00-000	NA	NA	NA
W*-143-Ti-002	0.20	0.17	<0.25
W*-144-Mo-001	0.0042	0.0044	<0.50
W-145-W-001	<0.15	<0.15	<0.15
W-146-Co-001	<1.70	<1.70	<1.70
W-147-N/Ni-002	0.40	0.33	<1.50
W-148-N/Mn-002	0.60	0.76	0.55
W-149-N/Fe-003	0.60	0.58	<1.50
W-150-N/V-003	0.03	0.03	<0.15
W**-151-00-000	NA	NA	NA
W**-152-Ti-001	0.2	Processing	<0.25
W-153-N/Ti-003	0.01	Processing	<0.25
W-154-N/Cr-003	0.55	Processing	Processing

* Low Resistivity p-type Ingots

** Use of double asterisk indicates 30 ohm-cm p-type ingot.